





## Article

# Automatic Proba-V Processor: TREX—Tool for Raster Data Exploration

Joanna Suliga <sup>1,\*</sup>, Joy Bhattacharjee <sup>2</sup>, Jarosław Chormański <sup>3</sup>, Ann van Griensven <sup>1,4</sup> and Boud Verbeiren <sup>1</sup>

<sup>1</sup> Department of Hydrology and Hydraulic Engineering (HYDR), Vrije Universiteit Brussels, Pleinlaan 2, 1050 Brussel, Belgium; Ann.Van.Griensven@vub.be (A.v.G.); Boud.Verbeiren@vub.be (B.V.)

<sup>2</sup> Water, Energy and Environmental Engineering Research Unit, Faculty of Technology, University of Oulu, Pentti Kaiteran katu 1, 90014 Oulu, Finland; Joy.Bhattacharjee@oulu.fi

<sup>3</sup> Department of Hydraulic Engineering, Warsaw University of Life Sciences, Nowoursynowska 166, 02-787 Warsaw, Poland; J.Chormanski@levis.sggw.pl

<sup>4</sup> Institute of Water Education, IHE-Delft, Westvest 7, 2611 AX Delft, The Netherlands

\* Correspondence: Joanna.Suliga@vub.be; Tel.: +32-2629-3036

Received: 13 September 2019; Accepted: 25 October 2019; Published: 30 October 2019



**Abstract:** The processing tool TREX, standing for ‘Tool for Raster data EXploration’ is presented and evaluated in the Biebrza wetlands in northeastern Poland. TREX was designed for the automatization of processing satellite data from the Proba-V satellite into maps of NDVI or LAI in any defined by the user projection, spatial resolution, or extent. The open source and access concept of TREX encourages the potential community of users to collaborate, develop, and integrate the tool with other satellite imagery and models. TREX reprojects, shifts, and resamples original data obtained from the Proba-V satellite to deliver reliable maps of NDVI and LAI. Validation of TREX in Biebrza wetlands resulted in correlations between 0.79 and 0.92 for NDVI data (measured with ASD Field Spec 4) and 0.92 for LAI data (measured with LiCOR—LAI-2000 Plant Canopy Analyzer).

**Keywords:** open source; free processing tool; NDVI; LAI; timeseries; Proba-V

## 1. Introduction

Launched in 2013, the Belgian satellite Proba-V provides free, global, and nearly daily observation coverage at various spatial resolutions (100 m, 300 m, or 1 km) [1]. This satellite sensor is capable of registering reflectance spectra in four bands (green, red and NIR, SWIR) that enables deriving one of the most popular remote sensing indices: the Normalized Differential Vegetation Index (NDVI). Timeseries of NDVI show changes in healthy green vegetation cover, thus allowing applications varying from environmental [2] and agricultural [3,4] to healthcare [5] or natural disasters monitoring [6]. Leaf area index (LAI), defined as a total one-sided green leaf canopy area per ground unit, is derivable from various remote sensing indices [7] including NDVI [8]. LAI, an index with a biophysical meaning, is used for improving classification e.g., of alkaline fen habitat [9] and for estimating agriculture productivity [10] or fluxes of transpiration [11] and interception [12]. LAI finds application in energy [13] or water balance-based modeling [14] where for instance in hydrological catchment models LAI determines interception capacity in relation to the beginning and the end of the growing season [15]. LAI maps derived directly from remote sensing can capture unexpected anomalies in foliage cover caused by for example fires, droughts, or deforestation. Dynamics of growing or degrading vegetation are often unpredictable thus difficult to properly represent in simulations without integrating this information from other sources like remote sensing.

LAI maps can be obtained from various sources ranging from manual processing of Landsat or Sentinel scenes, to acquiring ready-made products (for instance Copernicus—[www.land.copernicus.eu/](http://www.land.copernicus.eu/)

[global/products/lai](https://global/products/lai) or LSA SAF—[www.landsaf.ipma.pt](http://www.landsaf.ipma.pt)) or the real-time on-the-cloud editing service Mission Exploitation Platform (MEP) ([www.proba-v-mep.esa.int](http://www.proba-v-mep.esa.int)). For management or modeling purposes the spatial resolution is often an important element and thus Sentinel (10 m) or Landsat (30 m) are preferable over LAI maps from Copernicus Global Land Services (1/3 km or 1 km) or LSA SAF (1 km). On the other hand, the higher temporal resolution (1–2 days) of coarser products is a significant advantage (Landsat 8 revisit time is 16 days and Sentinel-2 is 5 days since the launch in 2017 of the second twin sensor). The cost of purchasing and the time needed for processing are important criteria regarding the selection of the best remote sensing products. Proba-V satellite was originally designed to provide 1/3 km or 1 km spatial resolution data via Copernicus Service however later were added and distributed via VITO product portal (<https://www.vito-eodata.be>) NDVI images of 100 m resolution. The 100 m spatial resolution maps combined with the almost daily revisit time of the Proba-V makes the product very interesting for ecohydrological modeling purposes. The Proba-V satellite that was just launched between the ending mission (March 2014) of SPOT Vegetation and planned Sentinel-1A (June 2015) and Sentinel-2B (March 2017) stands for a certain compromise between spatial and time resolution.

Various applications of NDVI and LAI often demands complex image processing which can be achieved using tools available either as open access (e.g., ILWIS, QGIS) or commercial (e.g., ArcGIS) GIS software. This way of processing images is a long chain of user-made decisions and thus quality highly depends on GIS skills or may lead to unintentionally obtaining various results from the same dataset. Less experienced users may also struggle with manually processing big data sets, especially when trying to utilize highly frequent satellite products like Proba-V that can provide up to 72 five-day synthesized NDVI maps per year. Proba-V images are synthesized from either 5 days or 10 days to overcome the issue of cloud cover but still missing data is a big challenge while manual processing. [1]. TREX (Tool for Raster data EXploration) is a processing tool designed for automatic processing hundreds of Proba-V images into maps with a user-specified spatial resolution, projection, and/or extent. If needed, TREX will also simulate NDVI values for no data pixels to construct complete maps.

TREX is an open source, highly automatic tool with many modules that is written in Python and provide the following advantages to other existing tools:

1. Reproducibility. User without advanced background in GIS can easily prepare any number of NDVI or LAI maps that will always, for the same settings, produce the same results;
2. Transparency. Open source approach reveals the exact code and processing chain allowing a collective collaboration on improvements;
3. Modularity. Advanced user can easily modify source code and add new features. The high level of automatization and the open source structure allows the tool to be easily coupled or integrated with other programs or cloud computation.

Within this paper, we present the TREX to public domain for carrying out research without involving advanced costly software, and we provide a demonstration and evaluation of its application to provide NDVI and LAI maps using Proba-V images in natural wetlands belonging to the Biebrza National Park in northeastern part of Poland.

## 2. Materials and Methods

### 2.1. TREX—Description of the Tool for Raster Data EXploration

TREX is a Python/GDAL open source and access tool designed for automatic processing raw Proba-V images into NDVI or LAI maps in an user defined projection, spatial resolution or extent. Structure of the TREX allows handling raster or vector data for any area, projection (if recognized by GDAL) or period after April 2014 (since Proba-V satellite data was available). Vector maps just like raster input and output data (delivered in ASC or TIF format) can be explored in any commonly used GIS software. Processing raw Proba-V images into final NDVI or LAI maps follows a strict automatic processing chain (shown in Figure 1) which includes:

1. Checking radiometric quality with the Proba-V Status Map (SM) and excluding processing images with too many invalid pixels (threshold defined by user);
2. Converting images from digital values to physical values;
3. Reprojecting maps based on the user input;
4. Resampling and fitting maps to a given grid based on the user input;
5. Clipping and masking out regions based on the user input;
6. Delivering NDVI maps in ASC or TIF format;
7. Computing LAI maps from NDVI maps;
8. Simulating value for missing pixels if enough information is available;
9. Delivering three types of LAI maps in ASC or TIF format: [1] LAI maps based on five-day synthesized NDVI map, monthly maps of average LAI with [2] or without [3] simulating missing data;
10. For selected points extracting timeseries of NDVI or LAI and saving in CSV format (readable by MS Excel);
11. Preparing and saving in PNG format visualization of LAI maps

The radiometric quality check of NDVI maps with the Proba-V SM allows a quick filtering of those maps which are containing too many invalid pixels. TREX allows a user to select a threshold and thus limiting the initial number of maps to the most informative scenes. Raw Proba-V images of NDVI consist of digital numbers (DN) which are translated into physical values (PV) based on the Equation (1) explained in the Proba-V manual [1]:

$$PV = \frac{(DN - offset)}{scale} \quad (1)$$

where PV is a value of NDVI; DN is a digital number ranging from 0 to 250 assigned to each pixel; offset and scale take a constant value of 20 and 250 respectively. TREX always processes all maps to match the exact properties of the input reference such as raster extent, masked values, projections, or spatial resolution using GDAL functionality. Automatic resampling is by default performed using the cubic method which can be easily modified within the open source code. Using the 'Reference Map' as input all selected images are clipped to the area of interest, potentially reducing the subsequent processing time and power needed significantly. The leaf area index (LAI) is computed from NDVI using the following Equation (2):

$$LAI = \sqrt{\left(NDVI \frac{1 + NDVI}{1 - NDVI}\right)} \quad (2)$$

LAI Equation (2) of Su [8] acts as an universal formula applied to all NDVI maps processed with TREX, having the advantage of always producing LAI values above 0. The flexible structure of the code allows integration of empirical equations for various crops or natural vegetation if enough data exists to establish accurate NDVI-LAI relation. Monthly maps of LAI are generated based on the aggregation of five-day synthesized maps whenever data is available. Due to the limited coverage of 100 m Proba-V (compared to 300 m and 1 km Proba-V) some areas are omitted or remain vulnerable to cloud, shadow or snow contamination thus, despite aggregation, some monthly maps may still contain pixels without valid data. Missing data can be simulated, based on a linear interpolation of the corresponding pixel values of the nearest two properly registered maps with data. If for the same pixel there are no values registered within the window of 5 months, then TREX replaces missing data with the mean value of all pixels from that month. The problem with missing data emerges especially during winter months when surface is covered with snow for a long time.

When processing NDVI and LAI maps is complete, TREX can extract timeseries of those parameters or automatically generate scaled maps. Delivering three types of LAI maps (single scene, monthly aggregation, or interpolated maps) allows the user to either accept missing data and continue vegetation

analysis based on the exact obtained information or accept a certain risk of interpolation but utilize complete maps of LAI. During processing TREX always reports the number of discarded scenes, number of simulated pixels per map etc. to inform the user about uncertainty. TREX also allows switching on and off certain elements of the processing chain to increase computation efficiency. TREX requires four types of input data:

1. Free Proba-V NDVI images obtained from the website (<https://www.vito-eodata.be>), preferable a 100 m product specified as 'S5-TOC—5-daily global composites, Top-Of-Canopy'; obligatory input
2. Each NDVI image should have an associated status map (SM) downloaded from the same website; obligatory input
3. A reference map in a TIF format. The extension, resolution, projection and masked areas within this file will be used for processing raw Proba-V images which means that all properties of output map will match with this reference map. Size and resolution of the reference map are only limited by processing capacity of a local machine; obligatory input
4. A point map in an SHP format. Each point should have specified an attribute named 'ID' which could be any number or name. The geographic projection of the point map and reference map must match; optional input

Executing the TREX script results in hundreds of outputs that can be grouped into:

1. NDVI maps (TIF or ASC format);
2. LAI maps: five-daily, monthly, or monthly including simulated missing data (TIF or ASC format);
3. Automated color representation of output maps (PNG format);
4. Timeseries of LAI and NDVI for selected plots and points;

The tool, source code, and short manual are freely available at the GitHub repository via the following link: <https://github.com/VUB-HYDR/TREX> (see Supplementary Materials). Running a script requires installation of GDAL and Python modules listed in the online manual.

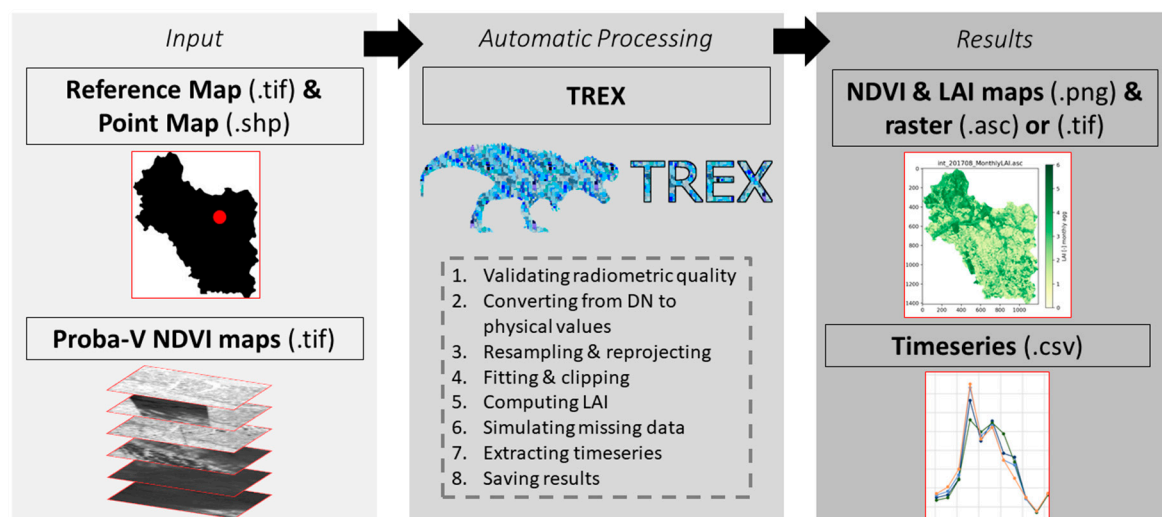


**Figure 1.** Generic scheme of TREX processing chain.

## 2.2. Case Study—Biebrza Valley

The study area of Biebrza wetlands was carefully selected based on available field data and knowledge which was used for critical evaluation of TREX. The area is a subject of ecohydrological studies for over 15 years resulting in obtaining well-documented and stable data. The presence of measuring tower equipped with two spectrometers and extensive fieldwork, covering multiple years and growing seasons, provide detailed validation data and greatly supports interpretation of the

results especially in the context of long term observations. Wetlands are also well acknowledged as a highly biodiverse ecosystem which provide wide range of vegetation types that can be used for evaluation of the use of one generic LAI equation.

Unique bog and fen wetlands located within the valley of the river Biebrza (195,000 ha) account to one of the most important ecological areas in Europe and thus resulting in the Biebrza National Park (BNP) being added to the Ramsar Convention list, EU Natura2000 network and European Life+ project. Due to high availability of water and nutrients, Biebrza wetlands are characterized by various habitats suitable for almost 300 species of birds and many extremely rare or close-to-extinction plant species [16]. The annual spring inundations [17] and groundwater seepage [18] formed rich peatlands of up to 3–6 m thickness [19] in the upper part of the river valley. Analyzed long term meteorological data, land cover maps and management practices indicated climatic changes and thus transition in vegetation schemes [20]. Observed encroachment of birch trees into wetlands locally increases transpiration and lowers groundwater levels thus creating a shift towards drier vegetation [21]. Triggered by varying water regime mineralization of the peat changes a gradient of productivity [22], eventually leading to irreversible changes in species composition and thus the functioning of the ecosystem [23]. Anthropogenic pressure, climatic changes, or natural succession are leading to degradation of Biebrza wetlands and therefore increasing the need for developing more advanced methods of environmental monitoring.

### 2.3. Evaluation Data from the Field

Data used for the evaluation of the TREX was collected during summer campaigns in 2015 and 2017. BNP is also the biggest national park in Poland. Therefore, for practical reasons, the sampling area was limited to wet meadows located in the Upper Biebrza valley. Sampling was conducted within 11 representative field plots containing four types of vegetation: pristine fen (plots PLP 3 and 4 shown in Figure 2), encroached wet meadows (PLP 4, 18, and 19), fen meadow (PLP 6, 7, and 16), and big sedge community (PLP 11). This selection of short vegetation (Figure 3) types provided various range of interesting sampling objects which were in the same time easier to measure than for instance high trees. Sampling procedure followed a very strict pattern presented in Figure 2. For each vegetation type one or more experimental plots (including 14 repetitions in total) with a size of  $8 \times 8$  m were established. Each plot was further subdivided into 16 smaller  $2 \times 2$  m areas ( $4 \text{ m}^2$ ) (Figure 2). Within each smaller subarea both spectral reflectance (with ASD Field Spec 4—analytical spectral devices) and LAI (with LiCOR—LAI-2000 Plant Canopy Analyzer or SunScan-Type SS1-COM-R4) were sampled. The thick, gray line visible in Figure 2 indicates the walking path inside the  $8 \times 8$  m grid, ensuring that, firstly the test object (vegetation) remains intact, secondly that all smaller subareas are accessible and thirdly prevents casting a shadow on a measured object. Clear sky is an important condition for acquiring reliable data and thus sampling could only be performed in specific days. Each plot (points A-B-C-D) was also measured with precise dual systems of dual frequencies GNSS receiver (GRS-1 by Topcon) using Real Time GNSS Reference Network Service TPI Net Pro (being a part of the world network TopNET Live) delivering high quality GPS/GLONAS correction data to rover receiver. This strict measuring pattern was applied to each plot during each campaign, which allowed the creation of a detailed and easily comparable dataset.



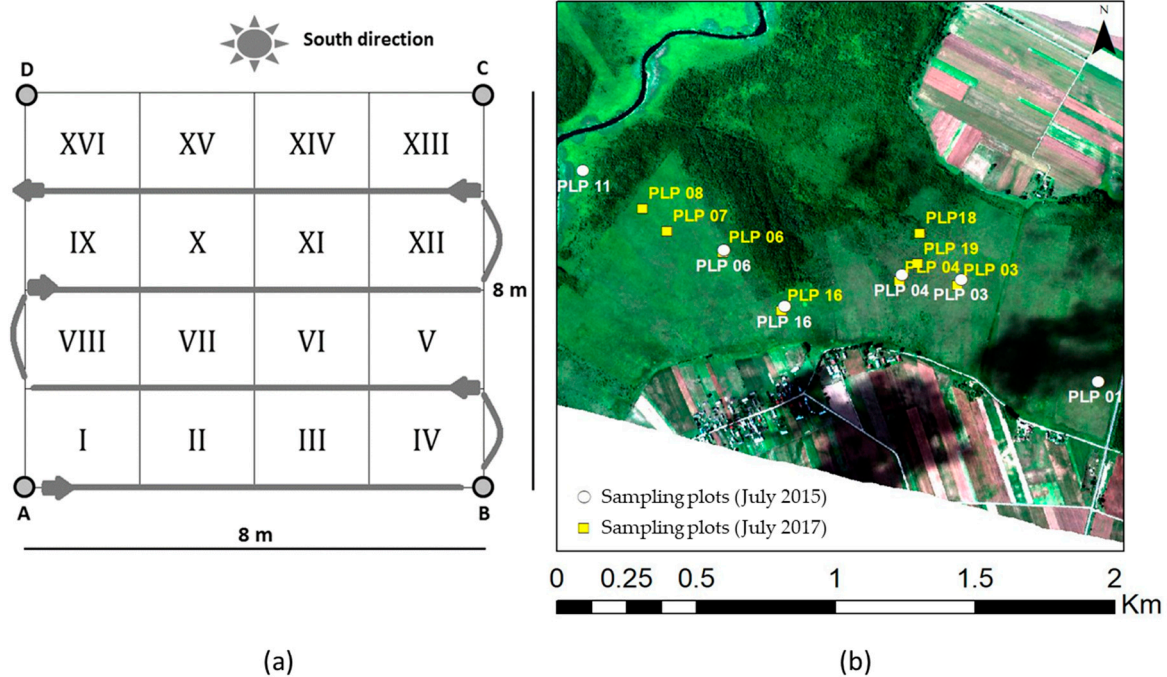


**Figure 2.** Measuring pattern of a single  $8 \times 8$  m sampling plot (a) and their location in the Upper Biebrza valley (b).

Additional validation data was obtained from two spectrometers installed on the tower located in the same study area (Figure 5). The time series of spectral reflectance were measured in the range of 400–1000 nm in about 0.2 nm intervals. Data collected by a set of two spectrometers USB2000+VIS-NIR (manufactured by Ocean Optics, Inc., Largo USA) looking forward and upwards with timestamp of 10 min were processed for obtaining one-per day reflectance curve, and finally narrow-band NDVI indices [24]. NDVI derived from RED and NIR bands of Proba-V are covering spectral ranges of 616–694 nm and 724–920 nm respectively thus to allow a proper comparison between ASD FieldSpec4, tower spectral data and satellite data, all measured spectra were aggregated to match exactly those ranges. NDVI was computed using a standard equation:  $NDVI = (NIR - RED)/(NIR + RED)$ . The wavelength accuracy of ASD Field Spec 4 is 0.5 nm for the wavelength range used in calculation.

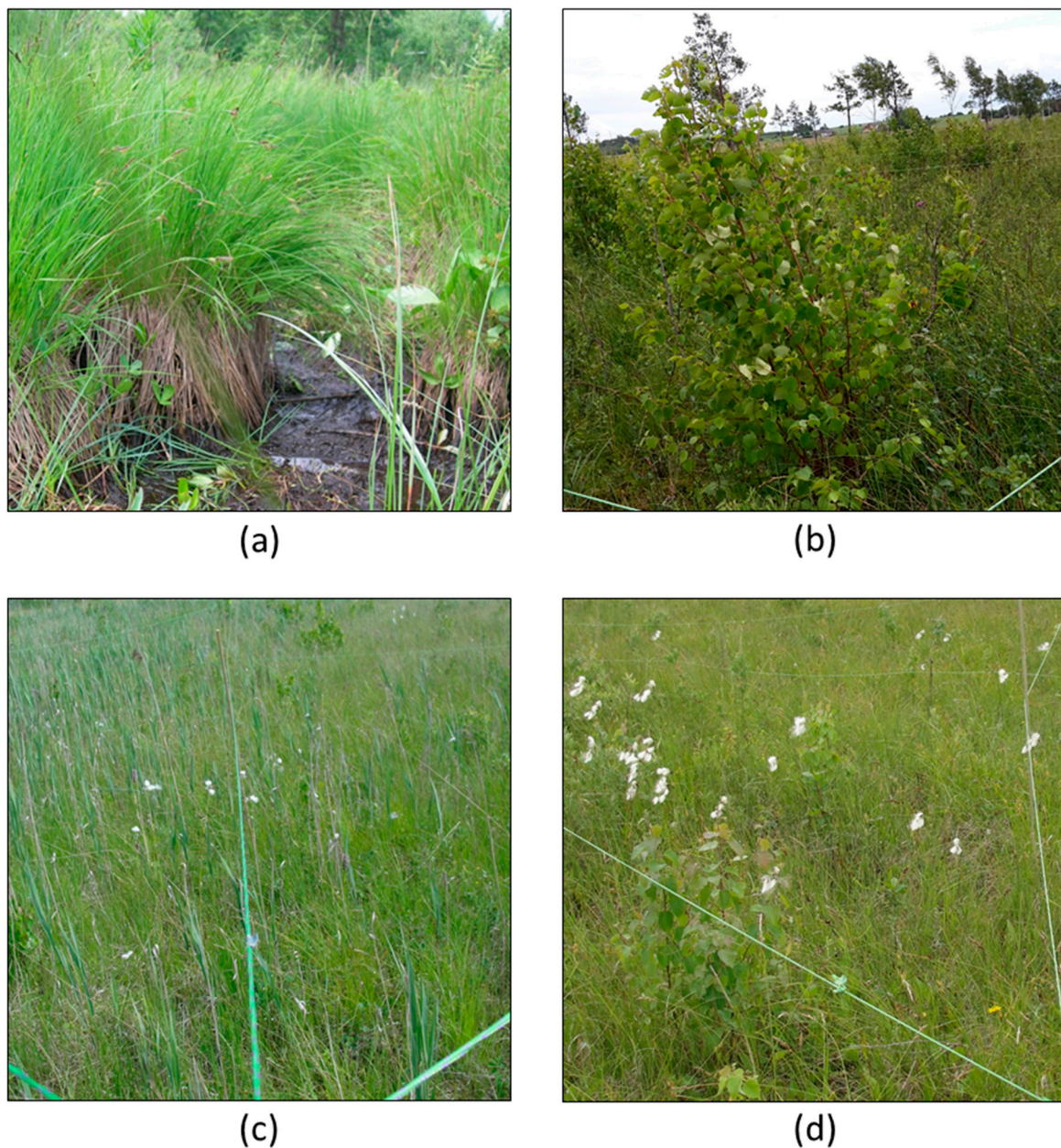


**Figure 3.** Pictures of vegetation present in the research area: big sedge communities (a), wet meadow encroached by birch trees (b), fen meadow—molinion (c), and pristine fen (d).

#### 2.4. TREX Application in Biebrza Wetlands

Six types of data inputs were used for TREX application to the Upper Biebrza valley (Northeast Poland):

1. Proba-V images of NDVI (and corresponding SM), five-day synthesis, TOC correction for the period April 2014–December 2017 (52 for year 2014 and 72 for each year 2015, 2016, and 2017), spatial resolution of 100 m;
2. A reference map of a small area located in the Upper Biebrza valley, spatial resolution of 30 m, size  $2 \times 10$  km, projected in UTM34N;
3. A point map with a several GPS points collected during field campaigns in July 2015 and 2017;
4. The hyperspectral image acquired on 16 of July 2015 using a sensor mounted on a plane with APEX system from VITO and BELSPO ([www.apex.vgt.vito.be/content/data](http://www.apex.vgt.vito.be/content/data)). For further analysis,

an image from a single flight line acquired at an altitude of 2500 m and at 15:26 local time was used. This 2 m spatial resolution image contained 285 spectral bands and covered an area of 20 km<sup>2</sup> (2 × 10 km);

5. The time series of meteorological data (temperature and precipitation) obtained from the Institute of Meteorology and Water Management (IMGW) in Poland;
6. The time series of spectral reflectance measured from the tower located in the study area. Spectral data was used for calculating NDVI using the exact same spectral range for red and NIR bands as for the Proba-V satellite.

Only the first three data sources were required for executing TREX script and producing NDVI/LAI maps or deriving timeseries of NDVI/LAI for selected points. APEX image (4), meteorological data (5), and spectral reflectance (6) were only used for analyzing the outcomes and explaining vegetation dynamics.

### 3. Results

#### 3.1. Mapping the Leaf Area Index (LAI) of Wetland Vegetation Types in Biebrza

Colorful maps are a quick way of previewing the outputs of processed images or to create animations (e.g., gif files) of LAI evolution over time. Figure 4 illustrates how well TREX (map c) output maps represent reality by providing a visual comparison between a true (b) and false (d) color map created from the high resolution (2 m) hyperspectral APEX image (acquired 14th of July 2015) and a single TREX map representing average LAI in July 2015. The upper image (a) in Figure 4 shows a zoomed area (red square) of 1 × 1 km corresponding to the one of the coarsest (also 1 × 1 km) available spatial resolution of the Proba-V sensor. Visible white lines represent the grid used in the reference map (30 m) thus showing how much information might be lost when coarse resolution images are used instead of 100 m Proba-V resampled and smoothed with TREX. The extent of the true color map (b) is matching the reference map thus showing a quick overview of the area and location of Biebrza river, dense forest (dark green), wet meadows (bright green), or agricultural land (light brown). The middle map (c) that shows average LAI in July 2015 was automatically generated with TREX using only Proba-V data of 100 m original spatial resolution and reference map (30 m). The false color composite (d) constructed from three bands (NIR, red, and green) utilizes vegetation properties to reflect more light in the NIR band than other materials. The lower map (d) exposes more variability within green vegetation areas which are otherwise less visible in a true color map (b). Especially coniferous forest mixed with bare soil (tiny blue stripes) in the lower right part of the map (d) stands out as deep dark red (almost brown) comparing to neighboring (from north) deciduous forest visible as red. Difference between reflecting properties of vegetation for red and NIR bands are utilized by NDVI index.



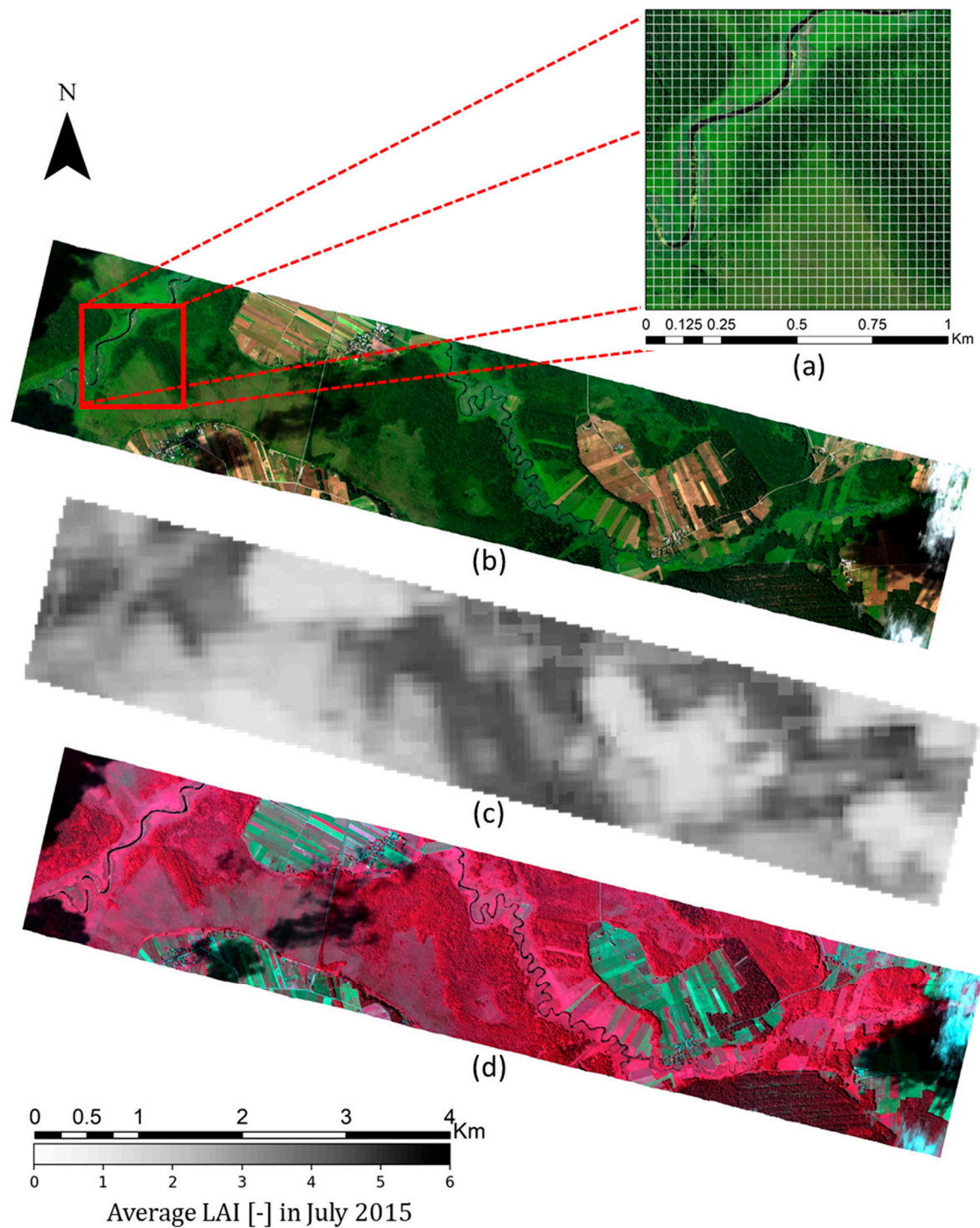


**Figure 4.** A comparison between true (b) and false (d) color map derived from the APEX image (2 m spatial resolution obtained on 16 July 2015) and a LAI (c) map (30 m spatial resolution computed based on average LAI for July 2015) processed with TREX. Top right map (a) is a zoomed area of 1 × 1 km with overlapped 30 m resolution grid.

### 3.2. Validating RS-Based Estimates from TREX with Field Measurements of NDVI and LAI

Using the coordinates of each point specified in the input vector map (shapefile), NDVI, and LAI timeseries values from corresponding pixels were extracted using TREX and compared with the corresponding field data collected during the summer campaigns in 2015 or 2017 (Table 1). NDVI and

LAI measurements from 2015 were well correlating with outcomes of the TREX processing (Table 2). In 2017 LAI samples, collected with the SunScan, were significantly lower than expected resulting in a poor correlation with the outcomes of TREX (Table 3—averaged by plot and Figure 5—all collected data from 2015 and 2017). SunScan device is designed in a way that sampling probe must be pushed under the vegetation canopy. Unfortunately, in the case of mossy vegetation that is covering 90% of the surveyed ground surface, SunScan was unable to measure tiny but densely growing plants, thus resulting in a high underestimation of LAI comparing to any measurement taken by a sensor located above the vegetation (for example mounted on UAV or satellite).

TREX is designed to utilize the finest resolution of the Proba-V satellite (100 m) that is not being used for producing and distributing LAI maps via the Copernicus Land Service. The research area was too heterogeneous (Figure 4) to provide a single  $333 \times 333$  m or  $1 \times 1$  km pixel with unified vegetation cover that could enable a comparison by vegetation class. Mission Exploitation Platform (MEP) is another service which is built around Proba-V data but in addition allows extraction of timeseries similar to TREX. MEP has great potential by at this moment timeseries of LAI for the research area were not available. Grid used by LSA SAF is coarse ( $1 \times 1$  km) and thus various of vegetation types are confused. One pixel contains all plots listed in the Table 1 and allowed extraction of LAI values equal to 3.3 in July 2015 and 5.0 in July 2017 (from LAI product synthesized from scenes obtained in the first decade of July).

**Table 1.** Summary of NDVI and LAI measurements conducted in July 2015 and July 2017 compared with the same values extracted from processed Proba-V images with TREX. Vegetation types: f—pristine fen; b—meadows encroached by birch trees; m—fen meadow (molinion); and s—sedge community.

Plot	Veg. Type	JULY 2015				JULY 2017			
		NDVI (ASD)	NDVI (TREX)	LAI (LiCOR)	LAI (TREX)	NDVI (ASD)	NDVI (TREX)	LAI (SunScan)	LAI (TREX)
		16.7.15	16.7.15	25.6.15	01.7.15	6.7.17	26.7.17	6.7.17	26.7.17
PLP 1	f	0.68	0.65	1.68	1.86				
PLP 3	f	0.68	0.68	1.72	2.01	0.75		1.3	
PLP 4	b			1.82	1.95	0.69		1.8	
PLP 6	m	0.71	0.79	1.66	2.41	0.67		1.6	
PLP 7	m					0.73	0.81	1.8	2.77
PLP 8	m					0.79	0.84	1.3	3.07
PLP 11	s	0.83	0.88	2.35	3.71				
PLP 16	m	0.75	0.79	1.78	2.39	0.78	0.8	1.8	2.65
PLP 18	b					0.83	0.85	1.7	3.23
PLP 19	b					0.74	0.78	2.3	2.54

**Table 2.** Correlation between field measurements (averaged by plot) from 16 July 2015 and maps processed with TREX using five-day synthesized image (16–20.07.2015)

	NDVI (ASD)	NDVI (TREX)	LAI (Li-COR)	LAI (TREX)
NDVI (ASD)	-	0.92	0.92	0.97
NDVI (TREX)	0.92	-	0.75	0.91
LAI (Li-COR)	0.92	0.75	-	0.92
LAI (TREX)	0.97	0.91	0.92	-

**Table 3.** Correlation between field measurements (averaged by plot) from 6 July 2017 and maps processed with TREX using five-day synthesized image (26–31.07.2017)

	NDVI (ASD)	NDVI (TREX)	LAI (SunScan)	LAI (TREX)
NDVI (ASD)	-	0.79	−0.16	0.81
NDVI (TREX)	0.79	-	−0.81	0.99
LAI (SunScan)	−0.16	−0.81	-	−0.73
LAI (TREX)	0.81	0.99	−0.73	-

### 3.3. Mapping LAI Dynamics of Wetland Vegetation with TREX

Left graph in Figure 5 shows a comparison between vegetation spectra measured by the tower (data available for 2 years) and four timeseries of LAI extracted from Proba-V images using TREX for the period of three years. Points I–IV used for data extraction are shown in the map present in Figure 5. Ecological studies carried in this area allowed to identify plots I and II as wet meadow and plots III and IV as meadow encroached by trees. High resolution imagery and meteorological data from IMGW (National Institute of Meteorology and Water Management) together with yearly visits and discussion with local managers explained the pattern of changing LAI of analyzed meadow. Biebrza Valley located in the continental climate zone has a broad range of changing temperatures during the year. Winters can be very cold with temperature sometimes reaching  $-20^{\circ}\text{C}$ , therefore the beginning of the growing season is very much dependent on the accumulated amount of snow and weather conditions during spring. Vegetation starts to grow in April–May and reaches climax (maximum) in June–July when also local managers cut the whole meadow for hay. A similar trend in Upper Biebrza valley was observed by Cieżkowski et al. [25] in his studies on interception canopy storage due an existing strong relation between LAI and interception capacity. Figure 5 shows that each sudden drops of LAI, linked to hay harvesting, was followed by another small peak of LAI which is explained by regrowth period. Late summer (August) can be dry or very hot (above  $30^{\circ}\text{C}$ ) and therefore hindering the capacity of vegetation to fully grow back. LAI in autumn continues to drop just like the temperature goes down, nights become longer, and vegetation season is about to finish. LAI curves also show the changing productivity of each sampling plot. Small spring flooding in 2014 made the meadow (point I) inaccessible for tractors, therefore mowing occurred later, when the soil dried up. 2016 was a very dry year, therefore area closer to the river had higher soil moisture and grew more (higher LAI) than vegetation located further away which was suffering from water stress.

Figure 5 also shows how spectral reflectance continuously measured with a spectrometer installed on a tower (located at point II) corresponds to other observations. Reflectance from the tower was processed and aggregated (daily) to derive firstly NDVI (same spectral ranges as Proba-V) and secondly LAI using the same universal equations of Su [8]. LAI estimations for point II from TREX (Proba-V maps of 100 m spatial resolution resampled to 30 m) were overestimated compared to point measurements collected at the tower location. Vegetation at the tower location is never used for hay production, therefore it is never cut (no rapid LAI drop in July); however, it follows seasonal changes thus showing decreasing trend in LAI towards the end of the season (2015).

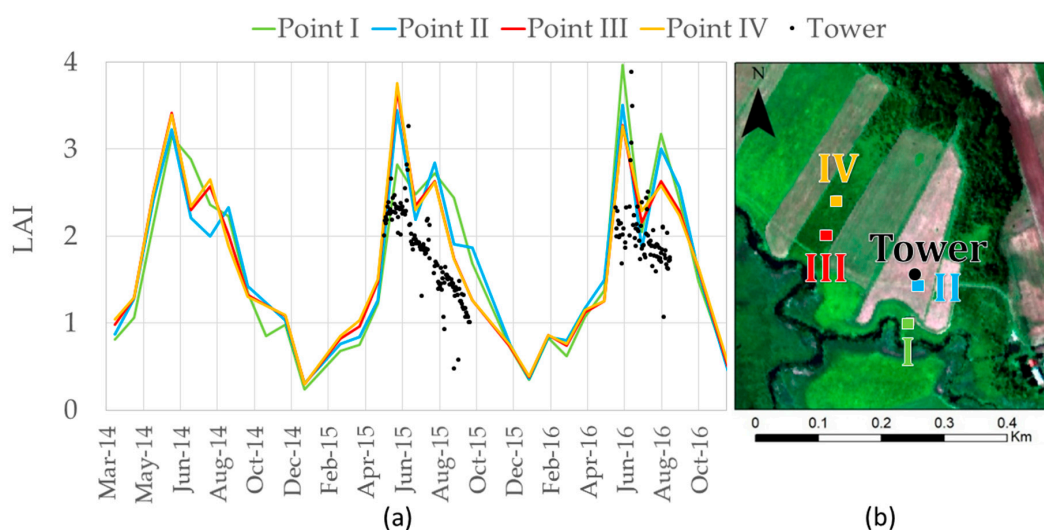


**Figure 5.** Comparison between the Tower data and Vegetation dynamics (a) captured with Proba-V and processed with TREX analyzed for 4 points (b) (from March 2014 until December 2016). Points I,II are representing wet meadows and III,IV meadows encroached by trees.

#### 4. Discussion

The open source algorithm and code TREX is targeting to provide automatic, uniform and reproducible NDVI or LAI maps and timeseries. Apart from typical GIS software (e.g., QGIS) similar results might be obtained from dedicated toolboxes like for example SNAP (successor of BEAM) from ESA or TSPT (Time Series Product Tool) from NASA. The added value of using timeseries of near-daily 100 m Proba-V NDVI estimates for mapping crops was proven successful in Sahelian and Sudanian Agrosystems [26] as well as in South America, Western and Eastern Europe [27]. The successful use of Proba-V NDVI timeseries for Spectral Matching Techniques (SMT) demonstrated in the work of Durgun [27] also showed the application of the well-developed SPIRITS software. This image processor, although powerful, is still based on user-made decision and thus creates a small niche for automatic processors such as TREX. The other advantage of TREX is that the code is written in Python, a programming language quickly gaining popularity amongst non-programmers (the third most used in 2018 programming language on GitHub repository). To overcome the low efficiency of the high-level language (Python) TREX is utilizing GDAL functions just like commercial ArcGIS. TREX and its users can greatly benefit from the simplicity of the Python language and the computation power of GDAL.

NDVI estimates of Proba-V satellite were often validated against predecessor mission of SPOT-V showing high correlation between both sensors [28–30]. Proba-V and SPOT-V showed high spectral consistency and almost 1:1 regression functions for blue, red, and NIR bands [28]. This is very important because the mission of the small Belgian satellite Proba-V will expire relatively soon, as this sensor was mainly designed to fill up the gap between the NDVI/LAI observations from SPOT-V and future Sentinel program. Due to its structure TREX can be harmonized with both SPOT-V and Sentinel and thus extends the analyzed period of available timeseries of NDVI/LAI from April 1998 until the end of Proba-V mission (2020 or later) and beyond. According to our knowledge very little work was done in testing NDVI product against data sampled directly in the field and for areas with diverse vegetation such as wetlands. A few LAI maps derived from Proba-V NDVI maps were successfully validated in the work of Wirion [14] for trees measured with SunScan.

An application of TREX in the Biebrza Valley gave satisfactory results although TREX automatic processing chain reprojects, shifts, and resamples all values from the original Proba-V images, the final outputs seem not to deviate from expectations. It is however highly recommended to take into consideration that the reliable spatial resolution of outcome maps is defined by the original resolution of input data. The cubic method of resampling images currently being used in TREX adds a smoothing effect to resulting maps therefore can well represent the natural vegetation transition and still produce accurate maps at higher resolution (30 m in this case) but may confuse highly heterogeneous semi-artificial areas (urban areas) where rapid changes in land cover occurs close to each other, e.g., asphalt road and lawn. Validation campaign by principle are very important for testing the quality of developed methodology. In this case, when mosses were dominating, SunScan struggled with producing reliable estimates of LAI, while Licor gave satisfactory results.

The very important flexibility of TREX enables the processing of maps for any area, providing various applications. For instance, TREX was used for monitoring productivity of date palms in Boudenib and Tafilalet oases in Morocco [31] by providing timeseries of LAI for a comparison with groundwater depth. The other application of TREX was a hydrological study on the role of the Doode Bemde wetland in the flood-prone Dijle valley where automatically processed Proba-V images were used in hydrological WetSpass model [32].

#### 5. Conclusions

This work demonstrates successful application of TREX in estimating NDVI (Pearson correlation between 0.79 and 0.92 with data measured with ASD—field spec) and LAI (correlation with Li-COR sampling device = 0.92) of Biebrza wetlands. Results obtained from TREX allowed temporal analysis of wetlands vegetation dynamics in form of timeseries or spatial analysis in form NDVI/LAI maps. LAI maps can be used in hydrological spatially distributed models to improve estimations of interception



processes through providing accurate information of vegetation development stage. The flexible structure of the code gives an opportunity to adapt NDVI-LAI relation equation based on field measurements, add NDVI/LAI—biomass estimation, or further analyze NDVI dynamics in time (anomaly detection). Although TREX is limited to Proba-V data set, it can be still adapted to accept maps from Sentinel or SPOT-V. The open source/access policy is meant to encourage the community to join and support further developments of the TREX tool.

**Supplementary Materials:** TREX is freely available at [www.github.com/VUB-HYDR/TREX](http://www.github.com/VUB-HYDR/TREX) including the installation manual. All results presented within this work can be reproduced using a reference map and two point maps available at [www.github.com/VUB-HYDR/TREX](http://www.github.com/VUB-HYDR/TREX) except for images of Proba-V NDVI and SM maps, which can be freely obtained from <http://www.vito-eodata.be/labeled> as product “S1 TOC 100 m [C1]”.

**Author Contributions:** A.v.G. and B.V. acquired research funding from BELSPO and coordinated the HiWET and WETMAN projects while J.S. applied for the ministerial permit in Poland. Sampling method was designed by B.V. and J.S. Field data acquisition was supervised by J.S. within the HiWET project except for the tower data obtained within the Intrev-WetEco project coordinated by J.C. The APEX and Proba-V images were processed by J.S. Concept and code of TREX was jointly developed by J.S., B.V., and J.B. Final version available on GitHub was prepared and uploaded by J.S. Processing data with TREX, validating, analyzing results, visualization, and writing the initial draft (including maps and graphics) was done by J.S. Reviewing was done jointly by A.v.G., B.V., and J.C.

**Funding:** This research was funded by the Belgian Federal Science Policy Office (BELSPO) within the HiWET (STEREO III Programme—SR/00/301) and WETMAN (STEREO III Programme—SR/03/369) projects.

**Acknowledgments:** We are thankful for the Polish government and director of the Biebrza National Park for granting us a permit to enter and conduct research in the protected areas of the Biebrza wetlands within the ministerial decision number DLP-III-4102-342/33577/15/md. We are also thankful for VITO and BELSPO for organizing the 2015 flight campaign with the APEX sensor. Special thanks we kept at the end for the Polish team that supported our yearly campaigns in Biebrza: thank you Sylwia, Tomasz, Małgosia, Wojtek, and Jarek.

**Conflicts of Interest:** The authors declare no conflict of interest. The funders had no role in the design of the study; in the collection, analyses, or interpretation of data; in the writing of the manuscript, or in the decision to publish the results.

## Abbreviations

TREX	Tool for raster data exploration
APEX	Airborne prism experiment
NDVI	Normalized difference vegetation index
LAI	Leaf area index
Proba-V	Project for onboard autonomy-vegetation
RS	Remote sensing
SM	Status map
TOC	Top of canopy
WetSpass	Water and energy transfer between soil plants and atmosphere

## References

1. Wolters, E.; Dierckx, W.; Iordache, M.-D.; Swinnen, E. *PROBA-V Products User Manual Document v3.01*; VITO: Boeretang, Belgium, 2018.
2. Gond, V.; Eva, H.; Cerutti, P.; Verhegghen, A.; Ceccherini, G.; Achard, F.; Gourlet-Fleury, S. The Potential of Sentinel Satellites for Burnt Area Mapping and Monitoring in the Congo Basin Forests. *Remote Sens.* **2016**, *8*, 986.
3. Roumenina, E.; Atzberger, C.; Vassilev, V.; Dimitrov, P.; Kamenova, I.; Banov, M.; Filchev, L.; Jelev, G. Single- and multi-date crop identification using PROBA-V 100 and 300 m S1 products on Zlatia Test Site, Bulgaria. *Remote Sens.* **2015**, *7*, 13843–13862. [[CrossRef](#)]
4. Zheng, Y.; Zhang, M.; Zhang, X.; Zeng, H.; Wu, B. Mapping winter wheat biomass and yield using time series data blended from PROBA-V 100- and 300-m S1 products. *Remote Sens.* **2016**, *8*, 824. [[CrossRef](#)]
5. Waldner, F.; Ebbe, M.; Cressman, K.; Defourny, P. Operational Monitoring of the Desert Locust Habitat with Earth Observation: An Assessment. *ISPRS Int. J. Geo Inf.* **2015**, *4*, 2379–2400. [[CrossRef](#)]

6. Klisch, A.; Atzberger, C. Operational drought monitoring in Kenya using MODIS NDVI time series. *Remote Sens.* **2016**, *8*, 267. [[CrossRef](#)]
7. Zheng, G.; Moskal, L.M. Retrieving Leaf Area Index (LAI) Using Remote Sensing: Theories, Methods and Sensors. *Sensors* **2009**, *9*, 2719–2745. [[CrossRef](#)] [[PubMed](#)]
8. Su, Z. Remote Sensing Applied to Hydrology: The Sauer River Basin Study. Ph.D. Thesis, Ruhr University Bochum, Bochum, Germany, 1996.
9. Kopeć, D.; Michalska-Hejduk, D.; Sławik, Ł.; Berezowski, T.; Borowski, M.; Rosadziński, S.; Chormański, J. Application of multisensoral remote sensing data in the mapping of alkaline fens Natura 2000 habitat. *Ecol. Indic.* **2016**, *70*, 196–208. [[CrossRef](#)]
10. Gitelson, A.A.; Peng, Y.; Arkebauer, T.J.; Schepers, J. Relationships between gross primary production, green LAI, and canopy chlorophyll content in maize: Implications for remote sensing of primary production. *Remote Sens. Environ.* **2014**, *144*, 65–72. [[CrossRef](#)]
11. Budny, M.L.; Benscoter, B.W. Shrub Encroachment Increases Transpiration Water Loss from a Subtropical Wetland. *Wetlands* **2016**, *36*, 631–638. [[CrossRef](#)]
12. De Jong, S.M.; Jetten, V.G. Estimating spatial patterns of rainfall interception from remotely sensed vegetation indices and spectral mixture analysis. *Int. J. Geogr. Inf. Sci.* **2007**, *21*, 529–545. [[CrossRef](#)]
13. Timmermans, W.J.; Kustas, W.P.; Anderson, M.C.; French, A.N. An intercomparison of the Surface Energy Balance Algorithm for Land (SEBAL) and the Two-Source Energy Balance (TSEB) modeling schemes. *Remote Sens. Environ.* **2007**, *108*, 369–384. [[CrossRef](#)]
14. Wirion, C.; Bauwens, W.; Verbeiren, B. Location- and time-specific hydrological simulations with multi-resolution remote sensing data in urban areas. *Remote Sens.* **2017**, *9*, 645. [[CrossRef](#)]
15. Suliga, J.; Chormański, J.; Szporak-Wasilewska, S.; Kleniewska, M.; Berezowski, T.; van Griensven, A.; Verbeiren, B. Derivation from the Landsat 7 NDVI and ground truth validation of LAI and interception storage capacity for wetland ecosystems in Biebrza Valley, Poland. In Proceedings of the SPIE 9637, Remote Sensing for Agriculture, Ecosystems, and Hydrology XVII, Toulouse, France, 22–25 September 2015.
16. Bartoszek, H. *Dolina Biebrzy*; Wydawnictwo Forest: Józefów, Poland, 2009.
17. Chormański, J.; Okruszko, T.; Ignar, S.; Batelaan, O.; Rebel, K.T.; Wassen, M.J. Flood mapping with remote sensing and hydrochemistry: A new method to distinguish the origin of flood water during floods. *Ecol. Eng.* **2011**, *37*, 1334–1349. [[CrossRef](#)]
18. Grygoruk, M.; Batelaan, O.; Okruszko, T.; Mirosław-Świątek, D.; Chormański, J.; Rycharski, M. *Groundwater Modelling and Hydrological System Analysis of Wetlands in the Middle Biebrza Basin*; Springer: Berlin, Germany, 2011; pp. 89–109. ISBN 978-3-642-19058-2.
19. Wassen, M.J.; Barendregt, A.; Pałczyński, A.; de Smidt, J.T.; de Mars, H. Hydro-ecological analysis of the Biebrza mire (Poland). *Wetl. Ecol. Manag.* **1992**, *2*, 119–134. [[CrossRef](#)]
20. Berezowski, T.; Wassen, M.; Szatyłowicz, J.; Chormański, J.; Ignar, S.; Batelaan, O.; Okruszko, T. Wetlands in flux: Looking for the drivers in a central European case. *Wetl. Ecol. Manag.* **2018**, *26*, 849–863. [[CrossRef](#)]
21. Grygoruk, M.; Batelaan, O.; Mirosław-Świątek, D.; Szatyłowicz, J.; Okruszko, T. Evapotranspiration of bush encroachments on a temperate mire meadow—A nonlinear function of landscape composition and groundwater flow. *Ecol. Eng.* **2014**, *73*, 598–609. [[CrossRef](#)]
22. Van Loon, A.H.; Schot, P.P.; Griffioen, J.; Bierkens, M.F.P.; Batelaan, O.; Wassen, M.J. Throughflow as a determining factor for habitat contiguity in a near-natural fen. *J. Hydrol.* **2009**, *379*, 30–40. [[CrossRef](#)]
23. Keizer, F.M.; Schot, P.P.; Okruszko, T.; Chormański, J.; Kardel, I.; Wassen, M.J. A new look at the Flood Pulse Concept: The (ir)relevance of the moving littoral in temperate zone rivers. *Ecol. Eng.* **2014**, *64*, 85–99. [[CrossRef](#)]
24. Cieżkowski, W.; Berezowski, T.; Kleniewska, M.; Szporak-Wasilewska, S.; Chormański, J. Modelling wetland growing season rainfall interception losses based on maximum canopy storage measurements. *Water* **2018**, *10*, 41. [[CrossRef](#)]
25. Cieżkowski, W.; Berezowski, T.; Kleniewska, M.; Chormański, J. Carbon Dioxide and Water Vapour Fluxes of a Alkaline Fen and Their Dependence on Reflectance. In Proceedings of the IGARSS 2018—2018 IEEE International Geoscience and Remote Sensing Symposium, Valencia, Spain, 22–27 July 2018; pp. 9253–9256.
26. Lambert, M.J.; Waldner, F.; Defourny, P. Cropland mapping over Sahelian and Sudanian agrosystems: A Knowledge-based approach using PROBA-V time series at 100-m. *Remote Sens.* **2016**, *8*, 232. [[CrossRef](#)]

27. Durgun, Y.Ö.; Gobin, A.; Van De Kerchove, R.; Tychon, B. Crop area mapping using 100-m Proba-V time series. *Remote Sens.* **2016**, *8*, 585. [[CrossRef](#)]
28. Dierckx, W.; Swinnen, E.; Kempeneers, P. Validation of spectral continuity between PROBA-V and SPOT-VEGETATION global daily datasets. *Int. Arch. Photogramm. Remote Sens. Spat. Inf. Sci. ISPRS Arch.* **2015**, *40*, 1155–1162. [[CrossRef](#)]
29. Sánchez, J.; Camacho, F.; Lacaze, R.; Smets, B. Early validation of PROBA-V GEOV1 LAI, FAPAR and FCOVER products for the continuity of the Copernicus global land service. *Int. Arch. Photogramm. Remote Sens. Spat. Inf. Sci. ISPRS Arch.* **2015**, *40*, 93–100. [[CrossRef](#)]
30. Meroni, M.; Fasbender, D.; Balaghi, R.; Dali, M.; Haffani, M.; Haythem, I.; Hooker, J.; Lahlou, M.; Lopez-Lozano, R.; Mahyou, H.; et al. Evaluating NDVI Data Continuity Between SPOT-VEGETATION and PROBA-V Missions for Operational Yield Forecasting in North African Countries. *IEEE Trans. Geosci. Remote Sens.* **2016**, *54*, 795–804. [[CrossRef](#)]
31. Badioui, K.; Suliga, J.; Huysmans, M.; van Griensven, A.; Verbeiren, B. Application of TREX script for vegetation monitoring in a Oasis Environment using Remote sensed data from ProbaV. *EGU Gen. Assem.* **2019**, *21*, 4318.
32. Bhatta, N. The Role of the Doode Bemde Wetland in the Flood-Prone Dijle Valley. M.Sc. Thesis, Vrije University Brussels, Ixelles, Belgium, 2018.



© 2019 by the authors. Licensee MDPI, Basel, Switzerland. This article is an open access article distributed under the terms and conditions of the Creative Commons Attribution (CC BY) license (<http://creativecommons.org/licenses/by/4.0/>).